Dalton Transactions

ROYAL SOCIETY OF CHEMISTRY

FRONTIER

View Article Online
View Journal | View Issue

Check for updates

Cite this: *Dalton Trans.*, 2026, **55**, 2015

# Beyond traditional electrocatalysts: polyoxometalates at the frontier

Zonish Zeb,[a,b,c] Md Maruf Ahmed,[d] Lubin Ni *[a] and Yongge Wei*[b,c]

Received 21st September 2025,
Accepted 29th November 2025

DOI: 10.1039/d5dt02256h

rsc.li/dalton

Intensified global energy demand and environmental concerns have made sustainable energy generation a global necessity. Water electrolysis and other processes, such as the $CO_2$ reduction reaction ($CO_2RR$) and nitrogen reduction reaction (NRR), are key green energy pathways that require efficient electrocatalysts with stability, multifunctionality, and structural diversity. Polyoxometalates (POMs) are exceptional due to their compositional diversity, structural versatility, active sites, and tunable electronic properties. However, challenges such as leaching, agglomeration, and low stability persist. In this frontier article, we focus on the exploration of POM-based and POM-derived materials for promising applications as electrocatalysts. We discuss advances in the POM materials (hybrids/derivatives) for electrocatalysis, with an emphasis on synthesis strategies, nanostructure design, and property enhancement through element doping, electronic modulation, heterojunction construction, morphological control, surface/interface engineering, and theoretical studies. We aim to summarize the current state of the art, highlight emerging trends, and provide insights into the future directions of POM electrocatalyst research to drive innovation in sustainable energy technologies.

Published on 01 December 2025. Downloaded on 3/14/2026 10:51:39 PM.

## Introduction

The depletion and adverse environmental effects of nonrenewable energy resources (oil and coal) with high carbon dioxide ($CO_2$) emissions are expected to increase to 36–43 Gt by 2035, urging a switch to renewable sources.[1] To combat these challenges, hydrogen ($H_2$), with a high energy density and zero emissions, presents itself as the fuel of the future. Water electrolysis, as an attractive approach, enables green $H_2$ production, whereas the $CO_2$ reduction reaction ($CO_2RR$) and nitrogen reduction reaction (NRR) offer complementary paths for carbon recycling and ammonia synthesis. However, the scalability of these reactions is hindered by high overpotentials and costly noble-metal electrocatalysts, which necessitate the fabrication of inexpensive, stable, and earth-abundant substitutes.[2] Polyoxometalates (POMs) represent an important class of metal oxides composed of elements such as V, Mo, Nb, Ta, and W, which display a unique diversity of structural, physical, and chemical features. POMs are strong electron-donating materials that participate in fast and reversible electron transfer reactions. Since their discovery nearly two centuries ago, POMs have unceasingly demonstrated novel structural architectures with solubility, redox activity, acidity, and thermal/chemical stability, expanding their scientific significance.[3–9] Furthermore, the electrochemical properties of POM nanostructures can be adjusted through material design strategies. These include regulating the metal composition, designing the molecular structure, modifying organic ligands, encapsulating in MOFs, and employing the heteroatomic atom engineering strategy.[10,11]

To date, abundant POM-based materials, including POM clusters, POM–MOFs (POM-contained metal–organic frameworks), and POM@Substrates (POMs deposited on conductive substrates), have been extensively explored for electrocatalytic water splitting, the $CO_2RR$, and other reactions.[12–18] Despite the significant progress, the POM-based materials face challenges, including inadequate structural stability under electrocatalytic conditions, low activity of bulk crystals, and poor electronic conductivity, all of which restrict their overall electrocatalytic performance.[19] Studies have indicated that the POM-based hybrids act as precursors for the development of transition-metal-based oxides, carbides, phosphides and sulfides, which are promising materials for the hydrogen evolution reaction (HER), the oxygen evolution reaction (OER), and other energy-related electrocatalytic applications.[10,20,21] In contrast to previous studies,[14–16,20] this frontier article highlights the

[a]*School of Chemistry and Chemical Engineering, Yangzhou University, Yangzhou, Jiangsu 225002, P. R. China. E-mail: lbni@yzu.edu.cn*
[b]*State Key Laboratory of Chemistry and Utilization of Carbon Based Energy Resources, College of Chemistry, Xinjiang University, Urumqi 830017, P. R. China*
[c]*Key Lab of Organic Optoelectronics & Molecular Engineering of Ministry of Education, Department of Chemistry, Tsinghua University, Beijing 100084, P. R. China. E-mail: yonggewei@tsinghua.edu.cn*
[d]*Institute of Innovation Materials and Energy, School of Chemistry and Materials, Yangzhou University, Yangzhou 225002, P. R. China*

Published on 01 December 2025. Downloaded on 3/14/2026 10:51:39 PM.

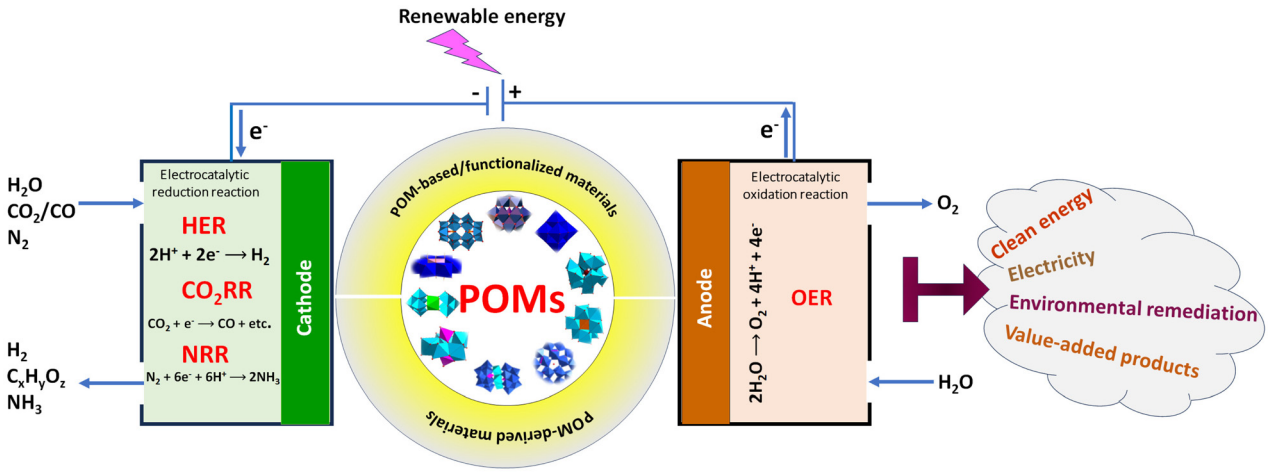


**Fig. 1** Schematic of the POM-based electrocatalysts driving the anodic OER with cathodic HER, $CO_2$RR, and $N_2$RR in an aqueous electrochemical system powered by renewable electricity.

role of POM materials in water splitting and other electrocatalytic applications (Fig. 1) by offering a guideline to construct POM materials from molecular scale to the industrialization. It emphasizes the construction strategies of POM materials, along with highlighting the importance of the theoretical studies and advanced characterization techniques to unlock the potential of the POM materials. The design strategies have been discussed systematically with structural evolution, electronic modulation, support interactions, and structure–property relationships. Finally, the current challenges have been addressed with future directions, aimed at directing future research to devise optimized POM materials with industrial-level current generation and stability while mitigating the drawbacks in electrocatalysis.

Different methods have been utilized to design new POM-based materials, including POM clusters, assemblies, organic–inorganic hybrids, and derivatives. These include room temperature, hydrothermal, solvothermal, ion exchange, chemical reduction, and electrodeposition synthesis methods. Furthermore, heat treatment methods for the POM derivatives include calcination, sulfidation, and phosphidation (Fig. 2).[22–26] Utilizing these methods, specific topics include the strategies for introducing the enhanced properties through element doping, the construction of heterojunctions, the modulation of electronic structures, the regulation of morphology and surface/interface engineering. Thus, the potential applications of the POM materials in electrocatalysis are discussed.

## Construction of the POM materials for electrocatalyst applications

POMs have been widely applied as electrocatalysts to facilitate the catalytic reactions.[12,27–29] The following sections highlight the strategies to achieve POM materials.

### POM-based/functionalized materials

POM-based materials can be categorized as POM single-cluster structures (inorganic assemblies and inorganic–organic hybrids) and POM nanostructures.[30,31] In POM-based hybrid materials, POM clusters are covalently, ionically, or coordinatively integrated with organic, inorganic, conductive, or polymeric components to combine the intrinsic catalytic, redox, and structural properties of POMs with the complementary functionalities of the host matrix.[32,33] These functionalization approaches address several key limitations of pristine POMs, such as high solubility in aqueous media and poor electrical conductivity, by stabilizing them in solid-state architectures and improving their processability.

**POM-based/functionalized materials for water splitting.** POM-functionalized hybrids exhibit excellent electrocatalytic properties for water splitting. Although POM superstructures with well-defined architectures hold great promise,[34] achieving controlled assembly for high-performance electrocatalysis remains a significant challenge.[16] A simple self-assembly strategy is employed to construct graphene-like POM-based superstructures, where transition metals (Co, Ni, or Cu) bridge POM clusters into ultrathin planes and cetyltrimethylammonium bromide (CTAB) acts as an intercalation agent, enhancing surface area and conductivity. Among the obtained materials (POM-CTAB-TM), POM-CTAB-Co exhibits the best OER activity, requiring an overpotential of only 292 mV to reach 10 mA $cm^{-2}$ with the lowest Tafel slope of 71.9 mV $dec^{-1}$. *In situ* spectroscopy and DFT (Fig. 3a) revealed that Co atoms and $\{Co_8Nb_{24}\}$ POMs facilitate the formation of a rapid electron-transfer pathway.[35] The exploration of crown ether-POM complexes represents a dynamic and fast-growing research area, offering innovative pathways for designing advanced supramolecular hybrid materials.[36,37] A novel crown ether–polyoxometalate hybrid assembly, $[Na(H_{24}C_{12}O_6)(CH_3CN)(H_2O)]_2[Na(H_{24}C_{12}O_6)(CH_3CN)_2][PW_{12}O_{40}]$ ($PW_{12}$@Crown), was successfully synthesized in an acetonitrile solution using Keggin-type

 This journal is © The Royal Society of Chemistry 2026

Published on 01 December 2025. Downloaded on 3/14/2026 10:51:39 PM.

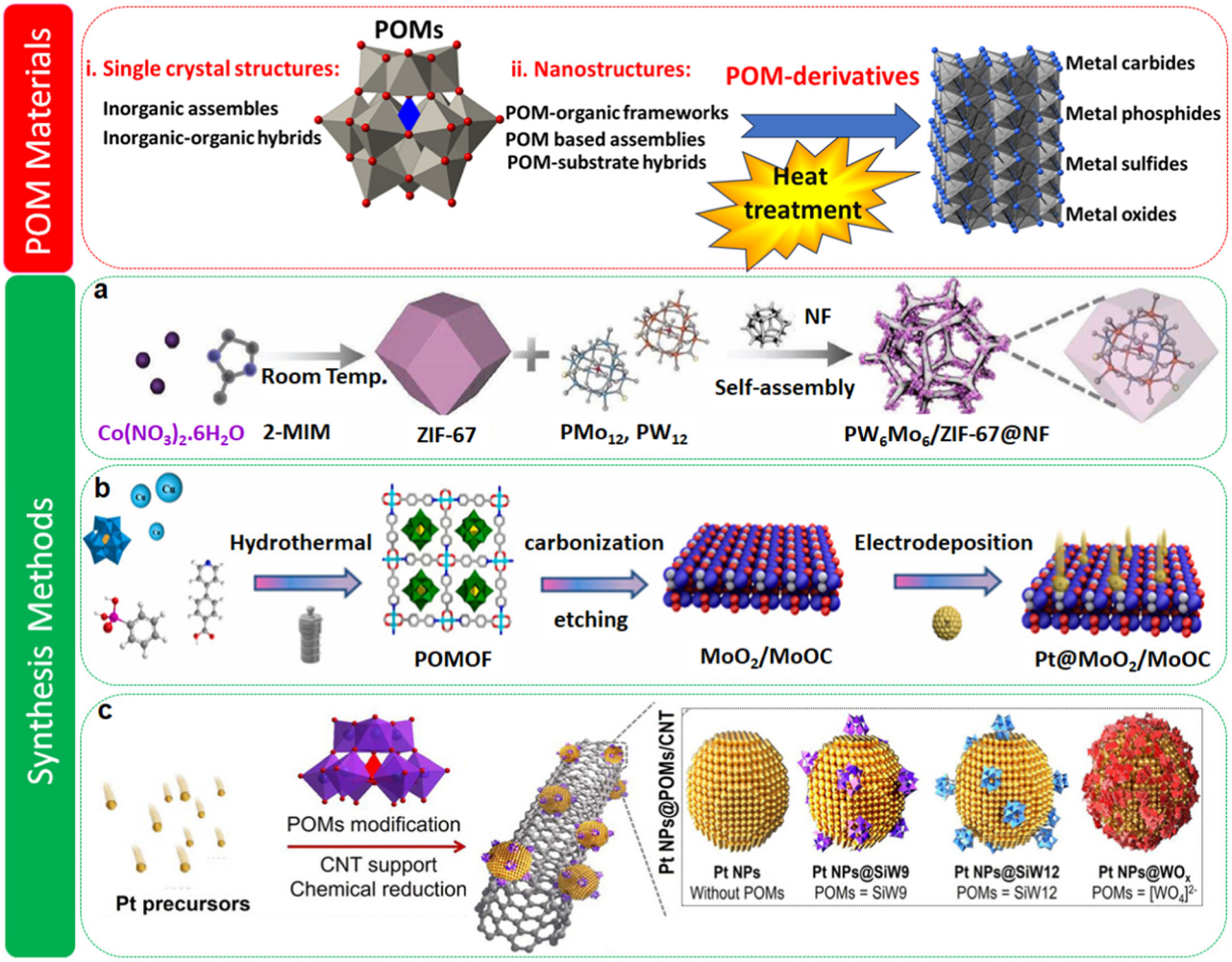


**Fig. 2** Categorization of the POM materials. Synthesis methods: (a) Room temperature synthesis. Reproduced with permission from ref. 22, with copyright permission 2024, Elsevier. (b) Hydrothermal method followed by carbonization and electrodeposition. Reproduced with permission from ref. 24, with copyright permission 2024, Elsevier. (c) Synthesis by chemical reduction and POM modification. Reproduced with permission from ref. 26, with copyright permission 2025, Wiley.

phosphotungstic acid. The structure was characterized by single-crystal and powder X-ray diffraction (PXRD) and was investigated for the HER. This supramolecular assembly represents the first example of a Keggin-type POM coordinated with three [18]-crown-6 ether moieties, forming a unique host–guest system stabilized by hydrogen bonding and other intermolecular interactions. The polyhedral stick-and-ball model of the crystal structures of the Keggin-type tungstate ($H_3[PW_{12}O_{40}]$) and its crown ether supramolecular compound ($PW_{12}$@Crown) is shown in Fig. 3b, and the polyhedral stacking structure is shown in Fig. 3c.[38]

However, POM-based compounds used as electrocatalysts for water splitting suffer from poor stability and conductivity during electrochemical reactions.[19] Integrating POMs with conductive materials improves leaching resistance and catalytic stability. This approach promotes heterogenization under electrocatalytic conditions, while simultaneously increasing the surface area and enhancing the electron transfer efficiency in water-splitting systems. The effective charge transfer between the POM catalysts and conductive substrates is vital for efficient HER and the multi-electron OER processes. A facile strategy for synthesizing Anderson-type POM-supported Cu dendrites ($NiMo_6O_{24}$@Cu/TNA) as efficient electrocatalysts for the HER in acidic media is presented. Enhanced $H^+$ transfer and H atom adsorption are achieved through the integration of $NiMo_6O_{24}$, resulting in a significant reduction in the overpotential by 130 mV and improvement of the stability.[39] A promising, low-cost route for a scalable energy conversion catalyst design is thus offered by this approach.

Graphene, a two-dimensional material, combines excellent conductivity and mechanical flexibility, enabling rapid electron transfer and uniform contact with the active species. These features improve charge transport, interfacial coupling, and stability, establishing graphene as an ideal support for high-performance and durable electrocatalysts.[40] The three-dimensional (3D) nano-assembly of nickel cobalt sulphide/

Published on 01 December 2025. Downloaded on 3/14/2026 10:51:39 PM.

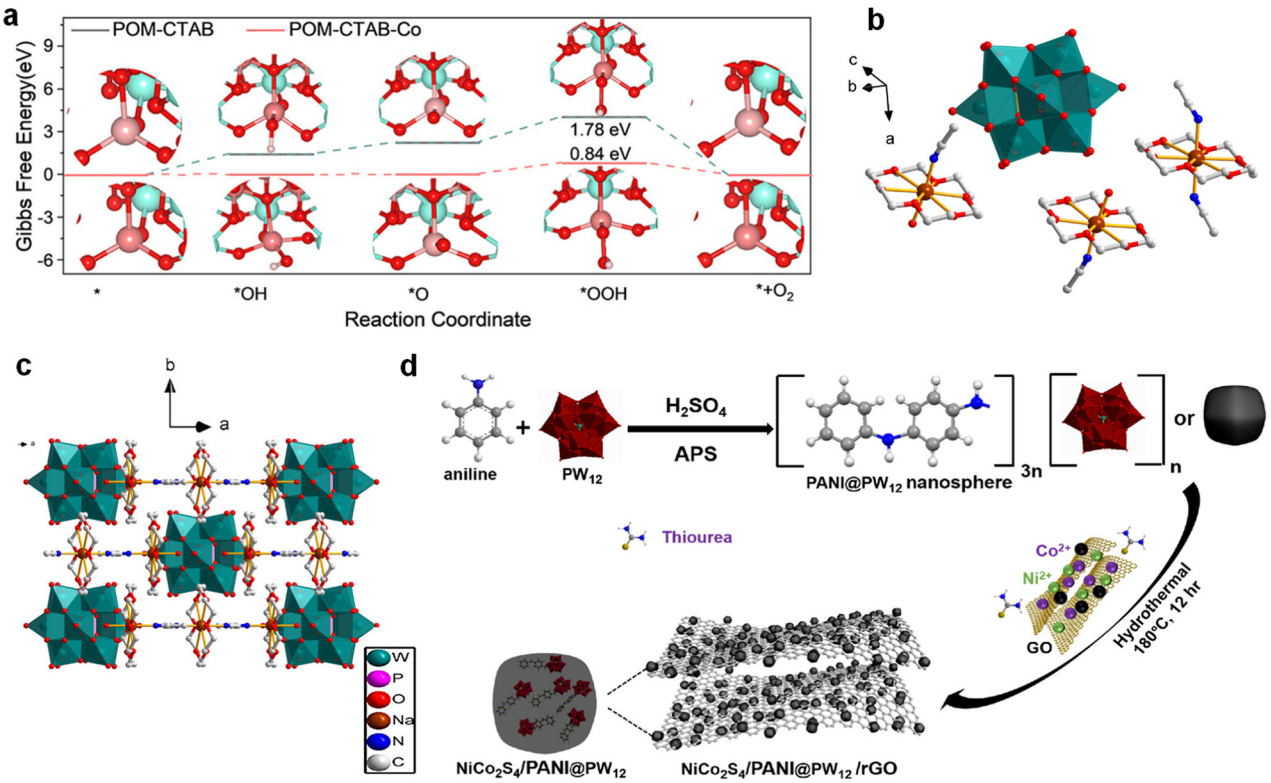


**Fig. 3** (a) Gibbs free energy diagram for the OER. Reproduced with permission from ref. 35, with copyright permission 2025, Wiley. (b) Polyhedral stick-and-ball model of the crystal structure of the Keggin-type tungstate ($H_3[PW_{12}O_{40}]$) and its crown ether supramolecular compound ($PW_{12}$@Crown). (c) Polyhedral stacking structure. Reproduced with permission from ref. 38, with copyright permission 2024, Elsevier. (d) Schematic of the synthesis route for $NiCo_2S_4$/PANI@$PW_{12}$/rGO. Reproduced with permission from ref. 41, with copyright permission 2022, Elsevier.

polyaniline @polyoxometalate/reduced graphene oxide ($NiCo_2S_4$/PANI@POM/rGO) was synthesized for the first time using a straightforward oxidative polymerization process, followed by a hydrothermal technique (Fig. 3d). The hybrid displayed sheet-like structures with uniformly distributed PANI@POM and $NiCo_2S_4$ on graphene, offering high structural integrity, large surface area, and abundant active sites. HER evaluation confirmed outstanding performance, featuring extremely low overpotential and remarkable long-term durability.[41]

Moreover, developing highly active and durable electrocatalysts for proton exchange membrane water electrolyzers (PEMWEs) operating at industry-relevant current densities remains a major challenge. At ampere-level current densities, the HER is hindered by the rapid interfacial proton depletion and sluggish kinetics. In this regard, anchoring tri-lacunary Keggin-type polyoxometalates on Pt enables proton-pump functionality and short-pathway hydrogen spillover, thereby overcoming interfacial proton depletion and the sluggish HER kinetics in PEMWEs. The as-optimized Pt NPs@SiW9 on the conductive carbon nanotube (denoted as Pt NPs@SiW9/CNT) delivered record mass activity (782.94 A $mg_{Pt}^{-1}$) with 6000 h durability at 2000 mA $cm^{-2}$ under ultralow Pt loading.[26] Thus, it offers a promising pathway toward next-generation low-Pt electrocatalysts utilizing POMs with conductive materials for practical PEMWE applications.

Developing and utilizing the distinctive heterostructures of POM with other materials might serve as an innovative approach to enhance the overall catalytic performance and durability of catalysts.[42] A POM incorporation strategy was employed to embed $PW_{12}$ nanoparticles into ZnCoS nanowires derived from ZnCo DHNWs *via* ion exchange (Fig. 4a). The SEM and TEM images (Fig. 4b–d) revealed relatively thick, rough, and short nanowires with $PW_{12}$ particles anchored on their surfaces. PXRD confirmed high crystallinity with characteristic peaks of $Zn_{0.76}Co_{0.24}S$ and $PW_{12}$ nanospheres, while Fourier transform infrared (FT-IR) spectra verified the $[PW_{12}O_{40}]^{3-}$ anchorage. The POM@ZnCoS nanohybrid grown on Ni foam exhibited superior OER and HER performance with the lowest Tafel slopes and remarkable stability in an alkaline electrolyte, outperforming commercial Pt/C and $RuO_2$ catalysts (Fig. 4e–h).[43] Additionally, a heterostructure composed of zinc iron oxide ($ZnFe_2O_4$) and POM nano plates (POM–$ZnFe_2O_4$) was fabricated using a hydrothermal method. The analysis of the HER and OER showed superior water splitting performance.[44] Considering these studies, the synergistic role of POMs with other materials in tailoring the electronic and atomic-scale properties is vital for the next-generation electrolyzer design. A cost-effective ZnFe LDH-$P_2Mo_{18}$/NF hybrid was synthesized *via* a simple hydrothermal method by integrating Wells–Dawson POM with ZnFe-layered double hydrox-

 This journal is © The Royal Society of Chemistry 2026

Published on 01 December 2025. Downloaded on 3/14/2026 10:51:39 PM.

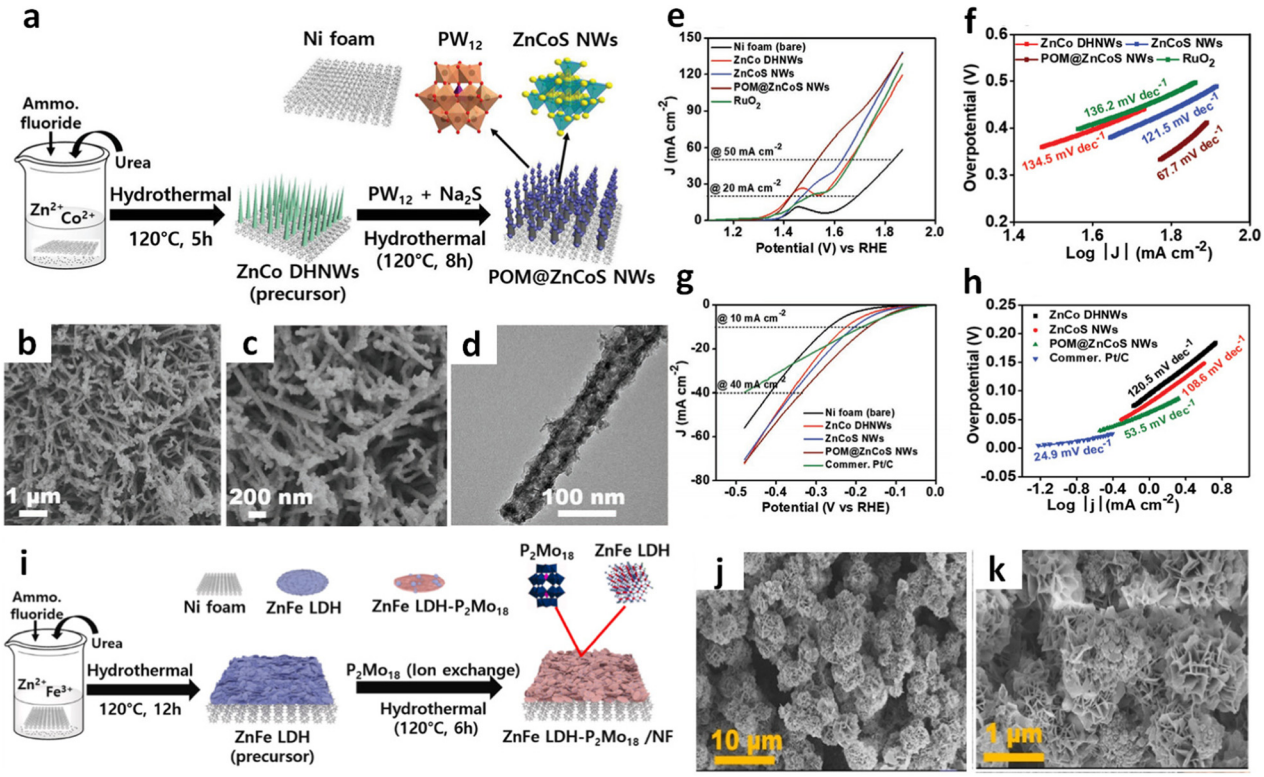


**Fig. 4** (a) Schematic of the synthesis process, (b and c) SEM images and (d) TEM images of the POM@ZnCoS NWs. Comparison of (e) LSV curves and (f) the corresponding Tafel slopes for the OER. (g) LSV curves and (h) the corresponding Tafel slopes for the HER. Reproduced with permission from ref. 43, with copyright permission 2022, Elsevier. (i) Schematic synthesis route of the ZnFe-LDH-$P_2Mo_{18}$/NF hybrid. (j and k) SEM images of the ZnFe-LDH–$P_2Mo_{18}$ hybrid. Reproduced with permission from ref. 45, with copyright permission 2023, Elsevier.

ide on the Ni foam (Fig. 4i). SEM images (Fig. 4j and k) revealed nanosheet arrays forming a porous hierarchical framework that promoted ion diffusion, electron transport, and electrode–electrolyte contact. This heterointerface engineering significantly boosted bifunctional HER/OER activity with low overpotentials through enhanced active sites and optimized electronic structures.[45] Moreover, a dual-field strategy combining $PW_{12}O_{40}^{3-}$ modification and electric field regulation promoted directional electron transfer, enabling $Ni(OH)_2$ to achieve an overpotential of 215 mV at 10 mA $cm^{-2}$ with a Tafel slope of 25.1 mV $dec^{-1}$ and remain stable over 100 h, outperforming $RuO_2$.[46] Through rational hybridization with conductive supports,[47] integration into porous metal organic frameworks (MOFs),[48–50] and coupling with transition-metal-based compounds, POMs can achieve enhanced electron transfer, structural robustness, and high active-site density for electrocatalysis.

**POM-based/functionalized materials for other applications.** Electrocatalytic $CO_2RR$ enables renewable energy storage and the production of value-added fuels like acetic acid. The electrocatalytic $CO_2RR$ of POMs was first reported by Kozik *et al.*[51] Since then, an increasing number of studies have focused on exploring the interactions between POMs and $CO_2$.[52,53] Our group reported a POM-modified copper nanocube catalyst forming Cu–O–Mo active sites, achieving 48.68% faradaic efficiency for acetate. DFT confirmed that these interfaces promote $*CH_3$ formation and $CO_2$ coupling, offering a model for designing efficient, earth-abundant POM-based $CO_2RR$ electrocatalysts.[54]

The electrocatalytic reduction of nitrite ($NO_2RR$) and nitrate ($NO_3RR$) to ammonia ($NH_3$) provides a sustainable pathway for $NH_3$ production while mitigating $NO_x$ pollution. Efficient catalysts are essential for this complex multi-electron process. POM-based hybrids markedly enhance $NO_2RR$ and $NO_3RR$ activity and durability.[55–57] For example, a tremella-like $P_8W_{18}$/CoNi-LDH electrocatalyst is developed *via* a simple hydrothermal-exfoliation method for efficient $NO_2^-$-to-$NH_3$ conversion, achieving a high $NH_3$ yield (0.369 mmol $h^{-1}$ $mg_{cat}^{-1}$) and 97.0% faradaic efficiency.[58] A novel Keggin-type POM crystalline complex was synthesized from a Waugh-type $[MnMo_9O_{32}]^{6-}$ precursor, representing the first reported conversion of a Waugh-type POM into a Keggin structure under hydrothermal conditions. The complex exhibited excellent stability and dual functionality, serving as an efficient electrocatalyst for $NO_2RR$.[59] These functionalization strategies not only boost activity in key reactions but also provide a versatile platform for designing tunable and durable electrocatalysts.

## POM-derived materials

**POM-derived materials for water splitting.** POM-derivatives, owing to their rich redox chemistry and unique properties,

Published on 01 December 2025. Downloaded on 3/14/2026 10:51:39 PM.

have been widely investigated as efficient catalysts for the HER, OER and overall water splitting.[60,61] A novel organoimido-derivatized heteropolyoxometalate (Mo4-CNP) was designed as a precursor (Fig. 5a and b), enabling *in situ* carburization, phosphorization, and atomic-level doping. This process yielded nitrogen-doped porous molybdenum carbide/phosphide hybrids with excellent HER activity.[62] The strategy highlights a promising route for developing highly active, non-noble metal electrocatalysts for hydrogen production.

To further address the stability and conductivity challenges, POM derivatives have been synthesized with various conductive substrates.[20,63,64] For example, the precise atomic engineering of nitrogen implantation into porous $Mo_2C$ nanocrystals was achieved through the straightforward pyrolysis of organoimido-derivatized POMs ($Mo_6$-nNAr) on a carbon fiber paper (CFP), a widely used conductive substrate (Fig. 5c). Combined experimental studies and density functional theory (DFT) calculations demonstrated that the inherently sluggish HER kinetics of the $Mo_2C$ catalysts could be significantly improved by nitrogen incorporation. This modification optimized the electronic structure of $Mo_2C$, producing favorable Mo–H binding strength and thereby delivering outstanding HER activity (Fig. 5d and e).[65] Further, using CFP, a tunable polyoxometalate-template-assisted strategy was used to atomically engineer metal doping sites on metallic 1T-$MoS_2$ with exceptional HER performance (−46 mV overpotential at 10 mA $cm^{-2}$, $\eta_{10(HER)}$), resembling that of platinum. Theoretical calculations confirmed that metal and oxygen co-doping facilitated water dissociation and hydrogen generation, offering a general approach to boost catalyst activity through targeted electronic modulation and atomic efficiency.[66]

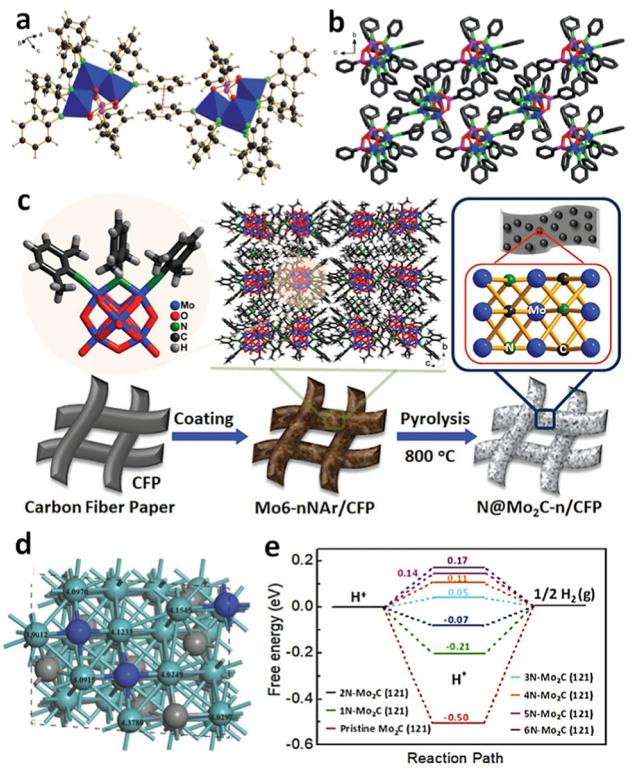


Fig. 5 (a) Weak π–π stacking interactions between adjacent Mo4-CNP molecules. (b) Packing structure of Mo4-CNP. Color code: Mo, blue; C, black; N, green; P, pink; O, red; H, gray. Reproduced with permission from ref. 62, with copyright permission 2018, Wiley. (c) Schematic of the synthesis process of N@$Mo_2C$-n/CFP. (d) DFT calculation results: the top view of 3N-$Mo_2C$ (121) and valence electron in the d-orbital of the surface-exposed Mo atoms. (e) The free energy diagram of the HER. Reproduced with permission from ref. 65, with copyright permission 2018, Wiley.

MOFs are organic–inorganic hybrids with metal centers linked by organic ligands, offering a high surface area and porosity. Thus, MOFs can serve as hosts to form POM-contained MOFs (POM–MOFs) to serve as ideal precursors for TM-based electrocatalysts.[67] With their fascinating structures, large specific surface areas, numerous catalytically active sites, and distinctive electrical and catalytic capabilities, the POM–MOF materials typically combine the benefits of both POMs and MOFs. They have extensive applications. Transition metal composites derived from POM–MOFs have particularly unique advantages of maintaining good overall morphology as well as the synergistic interaction of highly dispersed particles, which can avoid the poor stability drawbacks of crystalline POM–MOFs as catalysts, promote charge transfer, and provide more active sites.[30,31,68] A POM–MOF-assisted *in situ* confined conversion strategy was developed to synthesize octahedral molybdenum phosphide quantum dots embedded in porous carbon (MoP-QDs@PC) using a POM–MOF precursor ($PMo_{12}$@UiO-66), achieving high dispersion, conductivity, and a large specific surface area. The phosphorization-derived superhydrophilic MoP-QDs@PC exhibited exceptional HER performance, outperforming Pt/C at $\eta_{10(HER)}$ higher than 197 mV and 233 mV in alkaline and acidic media, respectively, due to an optimized electronic structure and enhanced wettability.[2] Recently, an Fe- and Mo-codoped NiS/$Ni_9S_8$ heterostructure on NF (Fe,Mo-NiS/$Ni_9S_8$/NF) was synthesized *via* interfacial engineering. First, $NiMo_6$@MIL-100 was prepared hydrothermally (Fig. 6a) and confirmed by PXRD (Fig. 6b) and $N_2$ adsorption/desorption (Fig. 6c). Hydrothermal sulfurization yielded the target catalyst, featuring abundant NiS/$Ni_9S_8$ interfaces with uniformly doped Fe and Mo atoms. The material exhibited ultralow OER overpotential at 10 mA $cm^{-2}$ ($\eta_{10(OER)}$) of 47 mV (Fig. 6d). Long-term chronopotentiometry (CP) testing in 1.0 M KOH at 1 A $cm^{-2}$ confirmed excellent stability for 90 h with negligible voltage change (Fig. 6e). Its performance was attributed to low interfacial resistance, abundant active sites, super-hydrophilicity, and strong electronic interactions.[69] This design strategy enables efficient water oxidation in challenging electrolytes.

Moreover, the use of the lacunary POMs provides vacant sites that can be utilized for the insertion of another metal; thus, the uniform dispersion of metal atoms can be achieved. For example, an efficient $Ni_3S_2$-$WO_3$/NF-1 electrocatalyst for water splitting was prepared using a lacunary POM precursor modified by vacancy-directed nucleophilic induction (Fig. 6f and g). Thus, the strategy guides the achievement of dispersed

 This journal is © The Royal Society of Chemistry 2026

Published on 01 December 2025. Downloaded on 3/14/2026 10:51:39 PM.

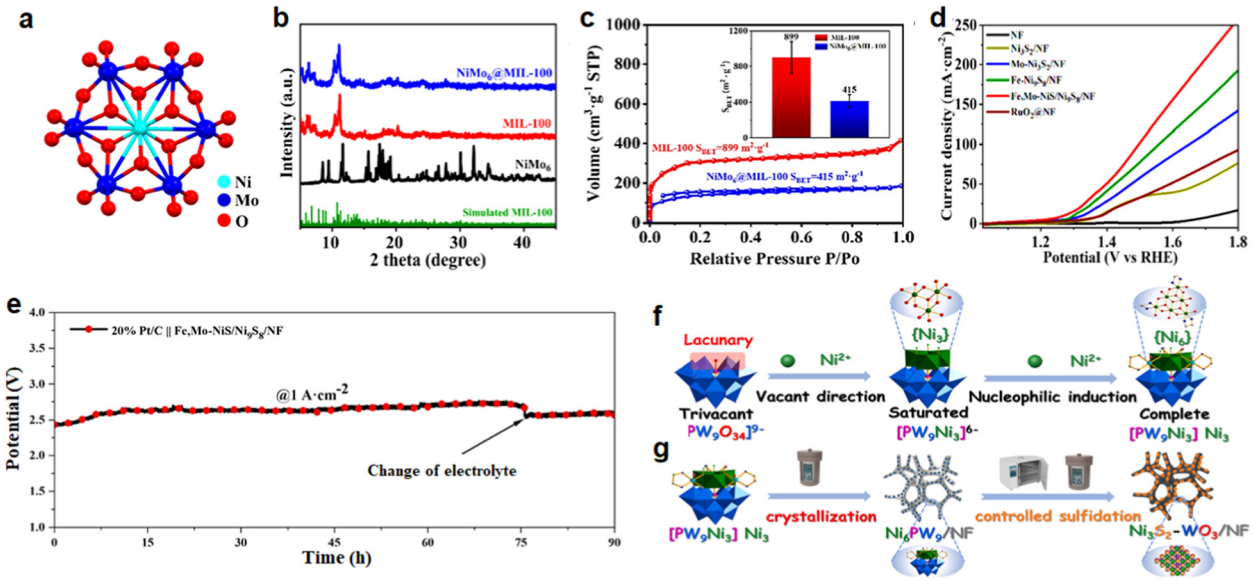


Fig. 6 (a) Structure of the $NiMo_6$ POM precursor. (b) PXRD pattern of $NiMo_6$, MIL-100, and $NiMo_6$@MIL-100. (c) $N_2$ adsorption/desorption isotherms of MIL-100 and $NiMo_6$@MIL-100. (d) OER activity in 1.0 M KOH. (e) CP curve of the Fe, Mo-NiS/$Ni_9S_8$/NF electrolyzer in 1.0 M KOH. Reproduced with permission from ref. 69, with copyright permission 2025, Elsevier. (f) Synthesis of $Ni_3S_2$-$WO_3$/NF-1. Reproduced with permission from ref. 70, with copyright permission 2023, Elsevier.

metal electrocatalysts for improved performance.[70] A comparison of the HER and OER performance of the POM-derived materials is given in Table 1.

**POM-derived materials for other applications.** The facile design of low-cost electrocatalysts is vital for efficient nitrogen reduction reaction (NRR); particularly, the POM-derived multiphase heterostructures show great promise.[68] A molecule-to-particle strategy using iron-oxo Keggin precursors yields Bi/BiClO/$Fe_3O_4$-600 composites with abundant active sites, porous structures, and enhanced conductivity. The catalyst achieved a high ammonia yield (12.82 μg $h^{-1}$ $mg_{cat}^{-1}$), 15.22% faradaic efficiency, and excellent stability at a low voltage.[75]

The current research on the POM derivatives for the $CO_2$RR is relatively inadequate. Extensive studies focusing on the synthesis of multimetallic POM derivatives with the deep integration of theoretical modeling are required. This will enable predictive control over electronic structures, surface energetics, and active-site configurations in POM electrocatalysts. Moreover, tailoring the interfacial chemistry, enhancing the long-term operational stability, and scaling the synthesis strategies are critical for transitioning POM materials from laboratory demonstrations to practical energy devices.

## Theoretical studies to underpin catalysis in the POM materials

Theoretical insight is essential for revealing interaction mechanisms, optimizing catalyst design, and correlating structural modifications with catalytic performance.[76,77] For example, a Lindqvist-type polyoxometalate ($[VW_5O_{19}]^{3-}$) cluster was used as a platform to investigate the catalytic performance of twenty-four transition metals solely *via* DFT calculations. Transition metals immobilized on the V-POM surface were considered as single-atom catalysts (SACs) and denoted as TMs@V-POM for simplicity. These results highlight that

Table 1 HER and OER performances of the POM-derived electrocatalysts

| Electrocatalyst | POM utilized | $\eta_{10(HER)}$ | $\eta_{10(OER)}$ | $Stability_{HER}$ (h) | $Stability_{OER}$ (h) | Electrolyte | Ref. |
|---|---|---|---|---|---|---|---|
| Pt@$MoO_2$/MoOC | $PMo_{12}O_{40}$ | 98.99 | — | 48 | — | 0.5 M $H_2SO_4$ | 24 |
| AlO@$Mo_2N$-NrGO | $AlMo_6$ | 111 | — | 300 | — | 1.0 M KOH | 25 |
| Co-h-$MoO_3$ | $CoMo_6$ | $130^*\eta_{100}$ | $359^*\eta_{100}$ | 120 | 60 | 1.0 M KOH | 60 |
| $CoMoO_4$ HTs | $PMo_{12}O_{40}$ | 75 | 210 | 60 | 72 | 1.0 M KOH | 61 |
| N@MoPCx-800 | $(TBA)_4[Mo_8O_{26}]$ | 108 | — | — | — | 0.5 M $H_2SO_4$ | 62 |
| NiO@1T-$MoS_2$ | $NiMo_6$ | 47 | — | 30 | — | 1.0 M KOH | 66 |
| Fe,Mo-NiS/$Ni_9S_8$/NF | $NiMo_6$ | — | 47 | — | 100 | 1.0 M KOH | 69 |
| $Ni_3S_2$-$WO_3$/NF-1 | $[PW_9O_{34}]^{9-}$ | 107 | $370^*\eta_{200}$ | 12 | 12 | 1.0 M KOH | 70 |
| Ru/Ni/WC@NPC | $Ni_{54}W_{72}$ | 3 | 75 | — | — | 1.0 M KOH | 71 |
| (Fe-$MoS_2$/$Ni_3S_2$@NF) | $\{Mo_{72}Fe_{30}\}$ | 74 | 80 | 10 | 10 | 1.0 M KOH | 72 |
| P-CoN/CMO/$Co_3O_4$/NF | $PMo_{12}O_{40}$ | 109 | — | ≥110 | — | 1.0 M KOH | 73 |
| $[Cu_{0.1}$-$\{MoO_2\}_{0.9}]$ | $[(Cu(pic)_2)_2(Mo_8O_{26})]\cdot 8H_2O$ | — | 374 | — | 18 | 0.5 M $H_2SO_4$ | 74 |

Published on 01 December 2025. Downloaded on 3/14/2026 10:51:39 PM.

V-POM, when functionalized with single transition-metal atoms, can serve as a highly effective support to significantly enhance HER electrocatalytic activity.[78] In addition, comprehensive DFT modeling for understanding the electronic and structural characteristics, as well as the overall influence, of adatoms on the polyoxotungstate (POT) cluster for water splitting and ORR was demonstrated.[79] Thus, POMs can exhibit impressive abilities in facilitating the water electrocatalysis. Looking ahead, the integration of DFT-guided predictions with innovative synthetic strategies will be central to unlocking the full potential of POM-based systems. By bridging theory and experiments, researchers can tailor the active sites with atomic precision, optimize electronic interactions, and design robust electrocatalysts for sustainable hydrogen production and beyond.

## Current challenges and future directions

Despite the significant progress in POM-based/derived electrocatalysts, several key challenges remain and need to be addressed. POM materials still show poor conduction, leaching, limited active sites, aggregation, structural instability, and complex synthesis methods for industrialization. POM–MOFs are ideal electrocatalysts, but uniformly embedding POMs in MOFs while maintaining strong interactions and structural integrity remains a challenge. In addition, ensuring strong POM-supported interactions, uniform dispersion, and stable charge transfer while identifying the active sites remains a key challenge for efficient electrocatalysis. In the POM-derived nanostructures, controlling morphology, composition, and phase evolution during formation is a current challenge. Moreover, there is limited research on understanding the comprehensive mechanisms of POM electrocatalysts, particularly how multi-metal interactions influence their electronic structure, performance stability, and selectivity.

In future research, comprehensive and well-designed strategies should be applied to address the above-mentioned challenges by (i) developing simple, scalable synthetic routes to facilitate the industrial application of POM electrocatalysts. Moreover, high-nuclearity POM precursors can be constructed by assembling polyanion units or incorporating heteroatoms to tune the electronic structures and accelerate charge transfer. (ii) The integration of POMs into porous matrices, such as MOFs, should be optimized to increase the surface area, promote heterogenization, and improve stability through strong POM-framework interactions. (iii) POMs should be integrated with the conductive substrates with enhanced binding abilities, and the structure–activity relationship should be studied to facilitate the charge transport and mitigate dissolution in different electrolytes. (iv) Multiple metals can be utilized in POMs with vacant sites as templates or precursors to synthesize nanostructured transition-metal compounds (*e.g.*, sulfides, phosphides, and carbides) with tunable composition, morphology, and interfacial coupling. (v) In addition, a mechanistic understanding is equally important. Advanced *in situ* and operando techniques[80] are indispensable for identifying active sites, probing intermediates, and monitoring dynamic structural and electronic transformations.

Together, these approaches would be beneficial to enhance electron/ion transport, increase active site density, improve durability, and elevate catalytic efficiency, thereby laying a solid foundation for the rational design of next-generation POM materials for industrial-scale electrocatalyst application.

## Conclusion

Polyoxometalate (POM) materials have emerged as promising electrocatalysts owing to their exceptional structural versatility, multi-electron redox capability, and molecular-level tunability. Despite these merits, key challenges remain. Establishing robust structure–activity correlations is essential for rational design, while preserving the intrinsic redox integrity of POM clusters under electrochemical operating conditions is critical to maintain their unique catalytic properties. Furthermore, stability at high current densities must be ensured to enable their deployment in practical applications. Moving forward, the synergy of innovative material design, theoretical modeling, and advanced characterization will be pivotal in developing robust, scalable POM electrocatalysts for sustainable hydrogen production and renewable energy applications.

## Author contributions

Zonish Zeb: conceptualization, writing – original draft, writing – review & editing; Md Maruf Ahmed: visualization; Lubin Ni: supervision, conceptualization, writing – review & editing, visualization, and funding acquisition; and Yongge Wei: supervision, conceptualization, writing – review & editing, visualization, and funding acquisition.

## Conflicts of interest

There are no conflicts to declare.

## Data availability

This is a frontier article based on publications in the literature. No primary research results, software or code have been included and no new data were generated or analyzed as part of this frontier article.

## Acknowledgements

This work was supported by the National Natural Science Foundation of China (No. 21971221, 22371158, 21225103, and 21401162), the Yangzhou University Interdisciplinary Research

 This journal is © The Royal Society of Chemistry 2026

Published on 01 December 2025. Downloaded on 3/14/2026 10:51:39 PM.

Foundation for Chemistry Discipline (yzuxk202010), the Natural Science Foundation of Jiangsu Province (BK20241930), the Qing Lan Project in Colleges and Universities of Jiangsu Province, and the Lvyangjinfeng Talent Program of Yangzhou.

## References

1 S. Meng, G. Li, P. Wang, M. He, X. Sun and Z. Li, *Mater. Chem. Front.*, 2023, **7**, 806–827.
2 Y. Liu, C. Yue, F. Sun, W. Bao, L. Chen, Z. Zeb, C. Wang, S. Ma, C. Zhang, D. Sun, Y. Pan, Y. Huang, Y. Lu and Y. Wei, *Chem. Eng. J.*, 2023, **454**, 140105.
3 G. Yang, Y. Liu and Y. Wei, *Coord. Chem. Rev.*, 2024, **521**, 216172.
4 D. Nowicka, N. Vadra, E. Wieczorek-Szweda, V. Patroniak and A. Gorczyński, *Coord. Chem. Rev.*, 2024, **519**, 216091.
5 J.-L. Lin, A. Zheng, Y. Xie, N. Chen, R.-L. He, B. Yin, W. Lv, Y. Wei and Y. Li, *Angew. Chem., Int. Ed.*, 2025, **64**, e202501763.
6 S. Li, Y. Zheng, G.-C. Liu, X.-H. Li, Z. Zhang and X.-L. Wang, *Polyoxometalates*, 2024, **3**, 9140061.
7 Q. Cai, R. Gao, Y. Wang, J. Xing, Q. Zhang, M. Zhu, X. Qin, M. Liao and Y. Huang, *Polyoxometalates*, 2025, **4**, 9140083.
8 P.-S. Wang, Z.-T. Wang, Y.-Y. Tan, P. Chen, X.-C. Zhang, L.-N. Zhang, Y.-G. Wei and L.-B. Ni, *Rare Met.*, 2024, **43**, 2241–2250.
9 S. Zhang, R. Liu, C. Streb and G. Zhang, *Polyoxometalates*, 2023, **2**, 9140037.
10 S. Zhu, H. Pang, Z. Sun, S. U. Khan, G. Mustafa, H. Ma, X. Wang and G. Yang, *Dalton Trans.*, 2024, **53**, 13248–13279.
11 L.-P. Cui, S. Zhang, Y. Zhao, X.-Y. Ge, L. Yang, K. Li, L.-B. Feng, R.-G. Li and J.-J. Chen, *Nat. Commun.*, 2025, **16**, 3674.
12 J. Ge, J. Hu, Y. Zhu, Z. Zeb, D. Zang, Z. Qin, Y. Huang, J. Zhang and Y. Wei, *Acta Phys. -Chim. Sin.*, 2020, **36**, 1906063.
13 Z. Zeb, Y. Huang, L. Chen, W. Zhou, M. Liao, Y. Jiang, H. Li, L. Wang, L. Wang, H. Wang, T. Wei, D. Zang, Z. Fan and Y. Wei, *Coord. Chem. Rev.*, 2023, **482**, 215058.
14 Z.-H. Wang, X.-F. Wang, Z. Tan and X.-Z. Song, *Mater. Today Energy*, 2021, **19**, 100618.
15 C. Freire, D. M. Fernandes, M. Nunes and V. K. Abdelkader, *ChemCatChem*, 2018, **10**, 1703–1730.
16 K. Li, T. Liu, J. Ying, A. Tian and X. Wang, *J. Mater. Chem. A*, 2024, **12**, 13576–13604.
17 K. Fu, L. Liu, P. Cui, X. Yan, Y. Wang and K. Chen, *Polyoxometalates*, 2025, **4**, 9140100.
18 Y. Zhang, Y. Liu, D. Wang, J. Liu, J. Zhao and L. Chen, *Polyoxometalates*, 2023, **2**, 9140017.
19 N. Li, J. Liu, B. X. Dong and Y. Q. Lan, *Angew. Chem., Int. Ed.*, 2020, **59**, 20963–20977.
20 T. Ma, R. Yan, X. Wu, M. Wang, B. Yin, S. Li, C. Cheng and A. Thomas, *Adv. Mater.*, 2024, **36**, 2310283.
21 C. F. Chen, A. P. Wu, H. J. Yan, Y. L. Xiao, C. G. Tian and H. G. Fu, *Chem. Sci.*, 2018, **9**, 4746–4755.
22 J. Song, P. Zhu, W. Ma and Y. Li, *Int. J. Hydrogen Energy*, 2024, **51**, 327–337.
23 S. Li, Z. Yang, Z. Liu, Y. Ma, Y. Gu, L. Zhao, Q. Zhou and W. Xu, *J. Colloid Interface Sci.*, 2021, **592**, 349–357.
24 S. Li, J. Liang, X. Tan, F. Li, X. Wang, L. Ma, L. Zhang and K. Cheng, *Int. J. Hydrogen Energy*, 2024, **51**, 1128–1137.
25 Y. Huang, W. Zhou, W. Kong, L. Chen, X. Lu, H. Cai, Y. Yuan, L. Zhao, Y. Jiang, H. Li, L. Wang, L. Wang, H. Wang, J. Zhang, J. Gu and Z. Fan, *Adv. Sci.*, 2022, 2204949.
26 H. Shen, Y. Huang, P. Zhao, R. Gao, Z. Wei, X. Gao, M. Liao, W. Dai, X. Liu, D. Sui, J. Liu, S. Zhu and Y. Wei, *Adv. Funct. Mater.*, 2025, e14862.
27 A. V. Anyushin, A. Kondinski and T. N. Parac-Vogt, *Chem. Soc. Rev.*, 2020, **49**, 382–432.
28 V. K. Abdelkader-Fernández, P. Garrido-Barros, M. Nunes and M. Gil-Sepulcre, in: *Applied Polyoxometalate–Based Electrocatalysis*, ed. D. M. Fernandes, John Wiley & Sons, Inc., 2025, pp. 183–218.
29 I. S. Marques, R. Matos and D. M. Fernandes, in: *Applied Polyoxometalate–Based Electrocatalysis*, ed. D. M. Fernandes, John Wiley & Sons, Inc., 2025, pp. 219–261.
30 K.-G. Liu, F. Bigdeli, A. Panjehpour, A. Larimi, A. Morsali, A. Dhakshinamoorthy and H. Garcia, *Coord. Chem. Rev.*, 2023, **493**, 215257.
31 Y.-R. Wang, Q. Huang, C.-T. He, Y. Chen, J. Liu, F.-C. Shen and Y.-Q. Lan, *Nat. Commun.*, 2018, **9**, 4466.
32 B. Fabre, C. Falaise and E. Cadot, *ACS Catal.*, 2022, **12**, 12055–12091.
33 Z. Wei, Z. Zeb, F. Abbas, Y. Wei and L. Ni, *Chem. – Asian J.*, 2025, **20**, e202500046.
34 K. Krishnamoorthy, P. Pazhamalai, R. Swaminathan, V. Mohan and S.-J. Kim, *Adv. Sci.*, 2024, **11**, 2401073.
35 R.-Z. Sun, X. Ma, K. Chen, J.-B. Yang, Y.-X. Liu, X.-X. Li, P.-W. Cai, Z.-H. Wen and S.-T. Zheng, *Angew. Chem., Int. Ed.*, 2025, e202513915.
36 G. Yang, Y. Wu, Z. Lv, X. Jiang, J. Shi, Y. Zhang, M. Chen, L. Ni, G. Diao and Y. Wei, *ChemComm*, 2023, **59**, 788–791.
37 J. Shi, H. Zhang, P. Wang, P. Wang, J. Zha, Y. Liu, J. Gautam, L.-N. Zhang, Y. Wang, J. Xie, L. Ni, G. Diao and Y. Wei, *CrystEngComm*, 2021, **23**, 8482–8489.
38 J. Shi, Z. Wang, J. Zha, P. Wang, P. Wang, X. Jiang, X. Liu, Q. Xu, X. Liu, G. Diao and L. Ni, *J. Mol. Struct.*, 2024, **1296**, 136831.
39 D. J. Zang, Y. C. Huang, Q. Li, Y. J. Tang and Y. G. Wei, *Appl. Catal., B*, 2019, **249**, 163–171.
40 M. A. Nazir, S. Afzal, I. Razzaq, L. Gurbanova, S. Ullah, I. A. Shaaban, A. Ahmad, A. Mohammad and S. S. A. Shah, *Int. J. Hydrogen Energy*, 2025, **161**, 150710.
41 J. Gautam, Y. Liu, J. Gu, Z. Ma, B. Dahal, A. N. Chishti, L. Ni, G. Diao and Y. Wei, *J. Colloid Interface Sci.*, 2022, **614**, 642–654.

Published on 01 December 2025. Downloaded on 3/14/2026 10:51:39 PM.

42 L.-p. Cui, Y.-w. Wang, K. Yu, Y.-j. Ma and B.-b. Zhou, *Adv. Funct. Mater.*, 2024, **34**, 2408968.
43 J. Gautam, Y. Liu, J. Gu, Z. Ma, J. Zha, B. Dahal, L.-N. Zhang, A. N. Chishti, L. Ni, G. Diao and Y. Wei, *Adv. Funct. Mater.*, 2021, **31**, 2106147.
44 J. Gautam, K. Kannan, M. M. Meshesha, B. Dahal, S. Subedi, L. Ni, Y. Wei and B. L. Yang, *J. Colloid Interface Sci.*, 2022, **618**, 419–430.
45 J. Gautam, P. Wang, A. N. Chishti, Z. Ma, Y. Liu, X. Jiang, J. Zha, L.-N. Zhang, G. Diao, Y. Wei and L. Ni, *J. Power Sources*, 2023, **581**, 233502.
46 K. Shi, W. Wu, Y. Zhao, S. Zhang, H. Jiang and G. Sun, *J. Alloys Compd.*, 2025, **1035**, 181610.
47 I. S. Marques, B. Jarrais, I.-M. Mbomekallé, A.-L. Teillout, P. de Oliveira, C. Freire and D. M. Fernandes, *Catalysts*, 2022, **12**, 440.
48 Y. Liang, H. Jiang, H. Lin, C. Wang, K. Yu, C. Wang, J. Lv and B. Zhou, *Chem. Eng. J.*, 2023, **466**, 143220.
49 V. K. Abdelkader-Fernández, D. M. Fernandes, S. S. Balula, L. Cunha-Silva and C. Freire, *ACS Appl. Energy Mater.*, 2020, **3**, 2925–2934.
50 V. K. Abdelkader-Fernández, D. M. Fernandes, S. S. Balula, L. Cunha-Silva and C. Freire, *J. Mater. Chem. A*, 2020, **8**, 13509–13521.
51 S. H. Szczepankiewicz, C. M. Ippolito, B. P. Santora, T. J. Van de Ven, G. A. Ippolito, L. Fronckowiak, F. Wiatrowski, T. Power and M. Kozik, *Inorg. Chem.*, 1998, **37**, 4344–4352.
52 Y. Cao, Q. Chen, C. Shen and L. He, *Molecules*, 2019, **24**, 2069.
53 C. Li, Y. Zhang, L. Shu, Y.-L. Teng, Y.-R. Wang and B.-X. Dong, *Polyoxometalates*, 2025, **4**, 9140097.
54 D. Zang, Q. Li, G. Dai, M. Zeng, Y. Huang and Y. Wei, *Appl. Catal., B*, 2021, **281**, 119426.
55 H. Lee, K.-H. Kim, R. R. Rao, D. G. Park, W. H. Choi, J. H. Choi, D. W. Kim, D. H. Jung, I. E. L. Stephens, J. R. Durrant and J. K. Kang, *Mater. Horiz.*, 2024, **11**, 4115–4122.
56 Z. Ni, N. Liu, C. Zhao and L. Mi, *Polyoxometalates*, 2024, **3**, 9140044.
57 H. Luo, X. Wang, Q. Jiang, G. Li, X. Ren, H. Pang and H. Ma, *Inorg. Chem.*, 2025, **64**, 21054–21066.
58 L.-N. Zhang, G.-A. Jia, C. Ma, M.-Q. Jia, T.-S. Li, L.-B. Ni and G.-W. Diao, *Inorg. Chem.*, 2024, **63**, 6787–6797.
59 P. Wang, A. N. Chishti, P. Chen, Z. Lv, Y. Tan, H. Zhang, J. Zha, Z. Ma, L. Ni, L.-n. Zhang and Y. Wei, *CrystEngComm*, 2022, **24**, 8134–8140.
60 Y. Wang, W. Shang, X.-t.-f. E, L. Zeng, X. Jia, N. Wang and Z. Jia, *New J. Chem.*, 2025, **49**, 9344–9353.
61 Z. Zhang, J. Ran, E. Fan, S. Zhou, D.-F. Chai, W. Zhang, M. Zhao and G. Dong, *J. Alloys Compd.*, 2023, **968**, 172169.
62 Y. Huang, J. Ge, J. Hu, J. Zhang, J. Hao and Y. Wei, *Adv. Energy Mater.*, 2018, **8**, 1701601.
63 M. Liao, Q. Zhu, Y. Li, Q. Yan, S. Zhou, J. Dai, Y. Huang and J. Gu, *Rare Met.*, 2025, **44**, 8609–8618.
64 W. Wang, M. Cai, T. Wang, S. Hou, X. Huang, Z. Wang, Z. Lu and P. He, *Adv. Mater. Technol.*, 2024, **9**, 2301607.
65 Y. Huang, J. Hu, H. Xu, W. Bian, J. Ge, D. Zang, D. Cheng, Y. Lv, C. Zhang, J. Gu and Y. Wei, *Adv. Energy Mater.*, 2018, **8**, 1800789.
66 Y. C. Huang, Y. H. Sun, X. L. Zheng, T. Aoki, B. Pattengale, J. E. Huang, X. He, W. Bian, S. Younan, N. Williams, J. Hu, J. X. Ge, N. Pu, X. X. Yan, X. Q. Pan, L. J. Zhang, Y. G. Wei and J. Gu, *Nat. Commun.*, 2019, **10**, 982.
67 J. Liu, M. Huang, Z. Hua, Y. Dong, Z. Feng, T. Sun and C. Chen, *ChemistrySelect*, 2022, **7**, e202200546.
68 X. Wang, Q. Jiang, M. Yang, H. Ma and H. Pang, *J. Alloys Compd.*, 2024, **1003**, 175786.
69 Z. Zeb, Y. Huang, L. Chen, R. Gao, X. Gao, M. Sun, H. Cai, J. Chen, F. Abbas, M. Liao, L. Ni and Y. Wei, *J. Colloid Interface Sci.*, 2025, **686**, 289–303.
70 F. Sun, C. Yue, J. Wang, Y. Liu, W. Bao, N. Liu, Y. Tuo and Y. Lu, *J. Colloid Interface Sci.*, 2023, **645**, 188–199.
71 A. Salah, L. Zhang, H. Tan, F. Yu, Z. Lang, N. Al-Ansi and Y. Li, *Adv. Energy Mater.*, 2022, **12**, 2200332.
72 T. Wang, B. Li, P. Wang, M. Xu, D. Wang, Y. Wang, W. Zhang, C. Qu and M. Feng, *J. Colloid Interface Sci.*, 2024, **672**, 715–723.
73 J. Ran, Z. Zhang, H. Feng, H. Zhao, D.-F. Chai, X. Huang, W. Zhang, M. Zhao, G. Dong, Y. Zang and S. Li, *Int. J. Hydrogen Energy*, 2024, **64**, 935–946.
74 P. Sood, Krishankant, H. Bagdwal, A. Joshi, K. K. Yadav, C. Bera and M. Singh, *ACS Appl. Nano Mater.*, 2024, **7**, 69–76.
75 X. Li, C. Xue, X. Zhou, Y. Wei, Y. Yu, Y. Fu, W. Liu and Y. Lan, *Mater. Chem. Front.*, 2023, **7**, 720–727.
76 M. R. Horn, A. Singh, S. Alomari, S. Goberna-Ferrón, R. Benages-Vilau, N. Chodankar, N. Motta, K. Ostrikov, J. MacLeod, P. Sonar, P. Gomez-Romero and D. Dubal, *Energy Environ. Sci.*, 2021, **14**, 1652–1700.
77 F. Abbas, Z. Wei and Y. Wei, *Adv. Theory Simul.*, 2025, e01185.
78 F. Abbas and Y. Wei, *Int. J. Hydrogen Energy*, 2025, **117**, 1–11.
79 F. Abbas, S. H. Talib, Z. Zeb, Z. Wei, S. N. Hussain, Y. Huang, S. Mohamed, A. Qurashi and Y. Wei, *Comput. Theor. Chem.*, 2025, **1244**, 115044.
80 Z. Wei, Y. Huang and Y. Wei, *Chem Catal.*, 2024, **4**, 101034.

 This journal is © The Royal Society of Chemistry 2026